

Enhanced relaxor behavior in epitaxial $\text{PbMg}_{1/3}\text{Nb}_{2/3}\text{O}_3$ films

M. Tyunina,^{1,*} J. Levoska,¹ D. Nuzhnyy,² and S. Kamba²

¹*Microelectronics and Materials Physics Laboratories, University of Oulu, PL 4500, FI-90014 Oulun yliopisto, Finland*

²*Institute of Physics, Academy of Sciences of the Czech Republic, Na Slovance 2, 182 21 Prague 8, Czech Republic*

(Received 11 January 2010; revised manuscript received 10 March 2010; published 28 April 2010)

Enhanced relaxor behavior in epitaxial $\text{PbMg}_{1/3}\text{Nb}_{2/3}\text{O}_3$ films are investigated. Analysis of the low-frequency intrinsic dielectric response is combined with studies of the response in far-infrared frequency range. The response is interpreted as that of a composite consisting of “matrix” and “dipoles.” Temperature dependence of the measured effective permittivity is explained by growth of the “dipolar” volume fraction on cooling. The dipolar relaxation time spectra are found to contain large fractions of fast relaxators, which increase with decreasing film thickness. This is shown to explain the enhanced relaxor behavior in the films. The peculiar fast dipoles are suggested to be influenced by film-substrate coupling.

DOI: [10.1103/PhysRevB.81.132105](https://doi.org/10.1103/PhysRevB.81.132105)

PACS number(s): 77.80.Jk, 77.80.bj, 77.55.Px, 77.22.Ch

Large dielectric permittivity and effective piezoelectric coefficient exhibited by perovskite-type relaxor ferroelectrics, or relaxors (REs), sustain device-oriented research of these materials. Also a great effort is directed to understanding fundamental atomistic and macroscopic features of REs responsible for their unique properties.¹ Compared to bulk ceramic or single-crystal REs, thin RE films are attractive for miniature devices but are much less studied and understood. In thin films, the small amount of material and the inevitable presence of extrinsic factors (such as substrate, electrode layers, etc.) prevent applying many experimental methods used for studies of bulk REs. However recently, the intrinsic low-frequency dielectric properties of epitaxial films of RE $\text{PbMg}_{1/3}\text{Nb}_{2/3}\text{O}_3$ (PMN) have been experimentally assessed.² Remarkably, they have been shown to noticeably differ from those of single-crystal PMN. In such films compared to bulk PMN, enhancement of RE behavior has been evidenced by a profound increase in the empirical scaling³ factor. In order to clarify possible mechanism driving epitaxial films toward “stronger” RE state, the low-frequency dielectric properties of epitaxial PMN films are analyzed in combination with analysis of their response in far-infrared (FIR) frequency range. The properties of epitaxial films are compared with those of single-crystal PMN (Refs. 4 and 5) and polycrystalline film.

The epitaxial PMN films of cubic perovskite structure, with (001) planes parallel to the substrate (001) surface, and with the cube-on-cube epitaxial relationship² were grown by *in situ* pulsed laser deposition. An $\text{La}_{0.5}\text{Sr}_{0.5}\text{CoO}_3$ bottom electrode layer and MgO (001) substrates (for the low-frequency studies) and also bare MgO (001) substrates (for the FIR studies) were used. For comparison, a polycrystalline PMN film was pulsed-laser-deposited on Al_2O_3 (0001) substrate using a thin SrTiO_3 buffer layer, similarly to that in Ref. 6. The low-frequency dielectric characterization of the vertical Pt/PMN/ $\text{La}_{0.5}\text{Sr}_{0.5}\text{CoO}_3$ /MgO capacitor heterostructures with pulsed-laser-deposited Pt top electrodes were performed using a Hewlett-Packard (HP) 4284A LCR meter and Linkam LTSE350 MultiProbe stage. The details of the growth, structural and dielectric characterization and identification of RE state can be found in Ref. 2. The amplitude of the probing ac field applied to the capacitors was 5–100 kV/m, considerably smaller than that at which changes in dielectric response of PMN films become detectable.^{2,7} The

FIR transmission spectra were acquired using a Fourier transform infrared spectrometer Bruker IFS 113 v, an Optistat (Oxford Instrument) cryostat, and a high-temperature cell Specac P/N 5850. A helium-cooled Si bolometer operating at 1.6 K was used as a detector. The details on the measurements and the fitting procedure can be found in Refs. 5 and 6.

At low frequencies, the real part of the dielectric permittivity measured in epitaxial PMN thin-film heterostructures, ϵ_H , differs from that in crystal. Unexpectedly, in contrast to the commonly observed decrease in ϵ_H in thin-film FE capacitors compared to FE bulk prototypes, a surprisingly large ϵ_H is obtained for PMN film thickness $d=750$ nm [Fig. 1(a)]. At temperatures $T > 400$ K and $T < 200$ K, the heterostructure exhibits ϵ_H which is *larger* than the permittivity in crystal measured at the same frequency. (Note that in vertical heterostructures, due to presence of a film-electrode interface capacitance, the measured effective permittivity is always smaller than that in the film.)

In PMN films, the temperature dependence of intrinsic permittivity ϵ (i. e. not affected by extrinsic factors such as

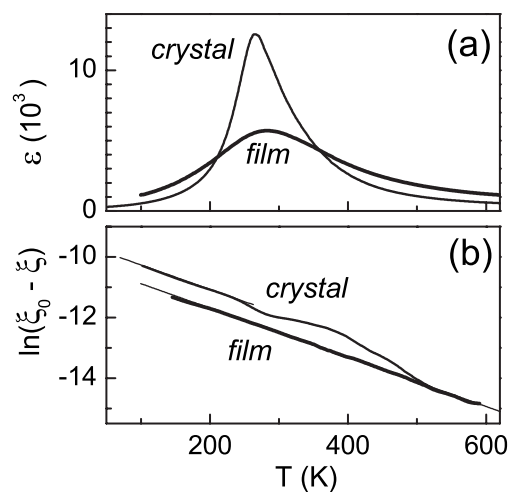


FIG. 1. (a) The dielectric permittivity ϵ as a function of temperature T measured at frequency $f=100$ kHz in the heterostructure of 750 nm thick PMN film and at $f=76$ kHz in the single-crystal PMN. (Ref. 4) (b) Verification of empirical expression (1) using the data from (a).

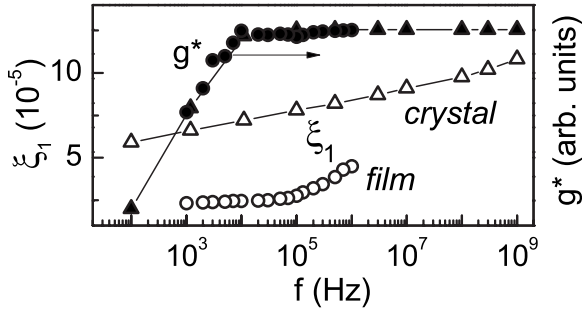


FIG. 2. The fitting parameter ξ_1 (open symbols) as a function of frequency f determined in PMN film at all T and in PMN crystal at low $T < 200$ K. The normalized relaxation spectra g^* are also shown (solid symbols).

electrodes, interfaces, and film conductance) at frequency f has been fitted by an empirical function²

$$\frac{1}{\varepsilon(f, T)} = \xi_0 T + \xi_1(f) \xi_2 \exp\left(-\frac{T}{\xi_2}\right) + I_0, \quad (1)$$

where ξ_0 , ξ_1 , ξ_2 , and I_0 are the temperature independent parameters. Using the derivative ξ of inverse permittivity: $\xi = \partial(\varepsilon^{-1})/\partial T$, it is easy to see that the expression (1) can be verified by analyzing the temperature dependence of $\ln(\xi_0 - \xi) = \ln \xi_1 - T/\xi_2$. The experimentally obtained linear temperature dependence of $\ln(\xi_0 - \xi)$ [Fig. 1(b)] proves validity of Eq. (1) for PMN films at T between 80 and 620 K. In PMN crystal, the behavior of $\ln(\xi_0 - \xi)$ is more complicated. However, at low T [below 250 K in Fig. 1(b)], the line is seen in the crystal too, with the parameters ξ_0 and ξ_2 being close to those in 750-nm-thick film.

The empirical expression (1) can be interpreted considering PMN film as a system of polar units, or “dipoles” embedded in a “matrix.” At very high $T \rightarrow \infty$, the inverse permittivity tends to that of matrix: $1/\varepsilon = \xi_0 T + I_0$. This only formally resembles the Curie-Weiss law for paraelectric state in FEs. The linear term $\xi_0 T$ in Eq. (1) suggests a paraelectric-like contribution present at *all* T . In the low- T limit $T \rightarrow 0$, the permittivity tends to $\varepsilon = 1/(\xi_1 \xi_2 + I_0)$, corresponding to a pure “dipolar” contribution.

The frequency dependent fitting parameter is ξ_1 (Fig. 2). All other experimental fitting parameters are found to be frequency independent. In PMN crystal, the parameter ξ_1 determined from the low- T derivative $\xi(T)$ depends on frequency f according to $\xi_1 \propto \log(f)$. In PMN films, another type of frequency dispersion $\xi_1(f)$ is found. In the low- T limit $T \rightarrow 0$, considering the frequency dependent permittivity being solely that of an ensemble of dipolar relaxators with a certain distribution $g(f)$ of relaxation times $\tau = 1/f$ and assuming $I_0 = 0$, the shape of the normalized relaxation spectra $g^*(f)$ can be evaluated

$$\varepsilon(f) = \varepsilon_{static} \int_{f_0}^f g(f) df \cong \frac{1}{\xi_1(f) \xi_2}, \quad (2)$$

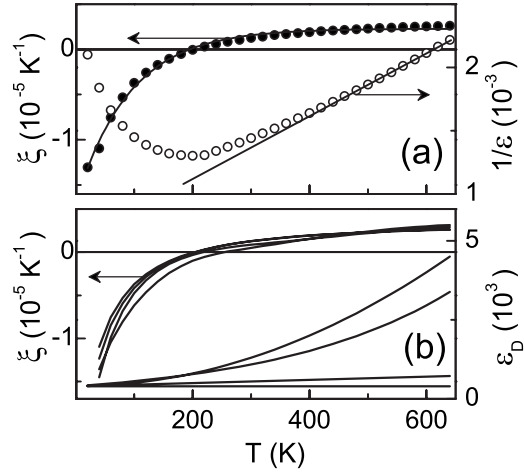


FIG. 3. (a) The inverse permittivity $1/\varepsilon$ (open symbols) and its derivative ξ (solid symbols) as a function of temperature T obtained by simulation in the two-component system with $c_M = 3 \times 10^5$ K, $T_D = 300$ K, and dipolar permittivity $\varepsilon_D = 400$. Linear fit to $1/\varepsilon$ mimics the Curie-Weiss law. Exponential fit to ξ agrees with expression (1). (b) The derivative $\xi(T)$ obtained in the system (a) with different temperature dependent dipolar permittivity (ε_D is also shown).

$$g^*(f) \cong -\frac{1}{[\xi_1(f)]^2} \cdot \frac{\partial(\xi_1)}{\partial f}. \quad (3)$$

In PMN film ($d = 750$ nm) and crystal at low T , the low-frequency edges of the normalized relaxation spectra g^* look similar (Fig. 2). For the films, however, the Vogel-Fulcher analysis has revealed that with decreasing film thickness, the average relaxation time becomes shorter.²

To understand physical meaning of the empirical expression (1) and of the fitting parameters therein, the permittivity of a two-component system including matrix and dipoles were considered. It can be roughly estimated using the Maxwell-Garnett equation⁸

$$\frac{\varepsilon - \varepsilon_h}{\varepsilon + 2\varepsilon_h} = v \frac{\varepsilon_i - \varepsilon_h}{\varepsilon_i + 2\varepsilon_h}, \quad (4)$$

where ε_h and ε_i are the permittivity of the dielectric host and spherical inclusions, respectively, and v is the relative volume fraction of inclusions. Using expression (4) the inverse permittivity $1/\varepsilon$ and its derivative ξ were numerically simulated for a fixed frequency. In simulations, a matrix with the permittivity c_M/T and $c_M = (0.1 - 10) \times 10^5$ K, and dipoles, the volume fraction v of which grows on cooling exponentially $v = \exp(-T/T_D)$ with $T_D = 100 - 500$ K were assumed. For $v < 0.5$, the dipoles were considered as inclusions and for $v > 0.5$ the matrix permittivity was treated as that of inclusions. The dipolar relaxation time spectrum and, hence, the dipolar permittivity were first assumed to be temperature independent. The dipolar permittivity ε_D was varied from 100 to 10 000. The results of simulations [Fig. 3(a)] qualitatively reproduce the dielectric response of PMN films. In the simulated temperature dependence of inverse permittivity $1/\varepsilon(T)$, the high-temperature linear part mimics the Curie-Weiss-type behavior. The simulated temperature dependence of deriva-

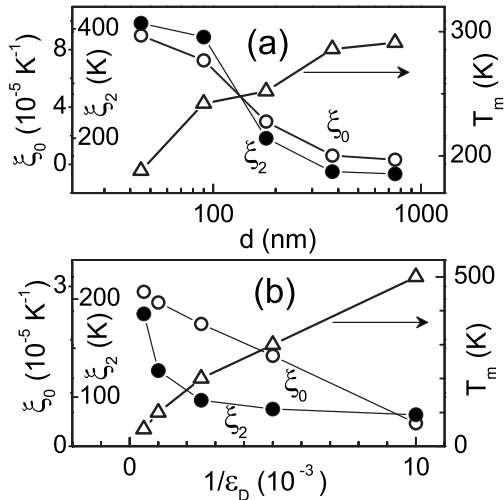


FIG. 4. The parameters ξ_0 and ξ_2 , and the temperature T_m of dielectric maxima (a) as a function of thickness d of PMN films determined from the experimental data (Ref. 2) and (b) as a function of inverse dipolar permittivity $1/\epsilon_D$ obtained by simulation in the two-component system.

tive $\xi(T)$ is fitted by an exponent: $\xi(T) = \xi_0 - \xi_1 \exp(-T/\xi_2)$, in excellent agreement with the empirical expression (1).

To simulate frequency dispersion of the response, the dipolar permittivity was varied in the limits of $\Delta\epsilon_D = 10\%$ around arbitrary ϵ_D from 100 to 5 000. The obtained corresponding variations in the temperature T_m of the dielectric peaks and of the fitting parameters are about $\Delta T_m \approx 7-9\%$, $\Delta\xi_0 < 2\%$, $\Delta\xi_1 \approx 8-12\%$, and $\Delta\xi_2 < 0.1\%$. Also these results reproduce the experimentally observed frequency dispersion of T_m and ξ_1 , with the parameters ξ_0 and ξ_2 being practically frequency independent.

To check an effect of temperature dependence of the dipolar permittivity $\epsilon_D(T)$ on temperature dependence of the total permittivity $\epsilon(T)$, the simulations were performed with the linear, polynomial, and exponential forms of the dependence $\epsilon_D(T)$ [Fig. 3(b)]. Also for the temperature dependent “dipolar” permittivity, the obtained derivatives $\xi(T)$ can be satisfactorily fitted by exponential functions.

The results of simulations and experimental observations imply that the main factor determining temperature dependence of the total permittivity $\epsilon(T)$ is the growth of the dipolar volume fraction on cooling. Remarkably, temperature evolution of the dipolar relaxation time spectrum has no considerable influence on the character of $\epsilon(T)$. Also the simulations show that the fitting parameters in expression (1) are connected to properties of matrix and dipoles in a complex manner and thus have no direct physical meaning.

In thin PMN films with decreasing thickness d , the fitting parameters of expression (1) are found to grow [Fig. 4(a)]. Such a growth leads to enhanced diffuseness of the intrinsic dielectric peaks. Previously, also shift of the temperatures T_m of the dielectric peaks to lower T has been found with decreasing PMN thickness.² Varying parameters in the above-described simulations (4) shows that the increase in the fitting parameters and the decrease in T_m are caused mainly by larger dipolar permittivity [Fig. 4(b)]. This qualitatively agrees with the found shorter average relaxation time, imply-

ing larger fraction of dipoles with short relaxation times, and correspondingly—larger fraction of dipoles contributing to the dipolar permittivity at a certain frequency.

The performed analysis of the low-frequency intrinsic permittivity suggests that the response of epitaxial PMN film can be thought as that of a two-component system, containing paraelectriclike matrix and dipoles. On cooling, the volume fraction of dipoles exponentially grows. This growth determines temperature dependence of the permittivity $\epsilon(T)$, which is practically unaffected by temperature evolution of the relaxation time spectrum and ϵ_D . In thinner films, dipolar relaxation spectra contain larger fractions of fast relaxators, with shorter relaxation times. This leads to increase in the low-frequency dipolar permittivity with decreasing film thickness. Consequently, the RE features in the dielectric response are enhanced.

Thus the peculiarity of epitaxial PMN films is the relatively large density of dipoles with short relaxation times. In perovskite-type bulk REs, the shortest relaxation time is known to be of the order of $10^{-12}-10^{-14}$ s, corresponding to FIR frequencies. To investigate the shortest-time edge of the relaxation spectrum in PMN films, FIR spectroscopy studies were performed.

In single-crystal PMN,^{4,5,9} at very high temperatures, the lowest polar phonon mode is believed to be connected with the formation of dynamic polar regions (corresponding to dipoles here). On cooling, the dielectric response of polar regions along the direction of local polarization becomes smaller than that in the orthogonal direction. Due to such an anisotropy, the soft mode splits into the low-frequency (20 cm^{-1}) E component and the high frequency A_1 component, which hardens on cooling below 500 K. The relaxational mode (or central mode) related to the dynamics of polar regions has been also detected at high T , where it overlaps with the E -mode.⁹ On cooling, however, the relaxational central mode slows to microwave and lower frequency ranges. At low $T \leq 50$ K, the presence of a mode near 65 cm^{-1} has been ascribed to possible changes in symmetry in the polar regions.^{6,9}

In the epitaxial PMN film on bare MgO substrate (PMN/MgO), the FIR transmission spectra were measured at different temperatures from 20 to 900 K. At all T , the phonon parameters of the film were determined below 100 cm^{-1} (Spectral limitation was due to absorption in MgO).¹⁰ The spectra fittings were performed for a two-layer system with the known phonon parameters of the substrate, which were separately investigated.

In the PMN/MgO film, the frequencies and the temperature evolution of the high- T soft mode and the A_1 -mode [Fig. 5(a)] are consistent with those in single-crystal PMN.^{4,5,9,11} The most obvious difference between the film and the crystal is seen in the heavily damped E -symmetry mode. In the film, its frequency is considerably higher, its phonon damping is about three times lower and its frequency is temperature independent. The behavior agrees with the presence of large density of fast dipoles revealed by the low-frequency dielectric analysis. The fastest dipoles are determined mainly by the E -mode phonons.

The epitaxial PMN films possess considerable degree of rock-salt type chemical B -site ordering.¹² To check if the

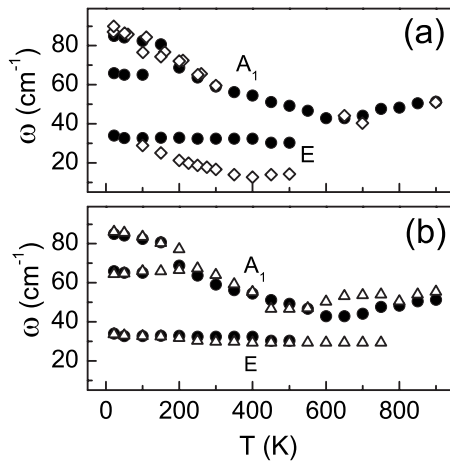


FIG. 5. Comparison of polar phonon frequencies ω observed in 500 nm thick (a) and (b) epitaxial PMN/MgO film (solid circles), (b) polycrystalline PMN/ Al_2O_3 film (open triangles) and (a) PMN single crystal (open diamonds) obtained using infrared spectroscopy (Refs. 6 and 9) and inelastic neutron scattering (Ref. 11).

peculiar E -mode is specific for epitaxial chemically ordered films only, the microstructure and the far-infrared spectra of a PMN film grown on $\text{Al}_2\text{O}_3(0001)$ substrate were investigated. The film was perovskite, polycrystalline, with random orientation of crystal planes relative to the substrate surface, and without a detectable (by x-ray diffraction) B -site ordering. The measurements and fitting of the spectra were similar to those in Ref. 6. Also in the polycrystalline PMN/ Al_2O_3 film [Fig. 4(b)], the heavily damped E -mode identical to that in the epitaxial PMN/MgO film is detected at $T = 20\text{--}750$ K.

Compared to single-crystal PMN in the studied PMN films, the dipoles exist at much higher T , their shortest relaxation times (corresponding to E -mode frequency) remain unchanged on cooling, and the density of the fastest dipoles is large (well above the experimental limit of detection) at all T .

The identical polar phonon structure observed in PMN/MgO and PMN/ Al_2O_3 films reveals negligible influence of

chemical ordering or epitaxial quality on fast dipoles. It is worth mentioning that studies^{6,13} of single-crystal, ceramic, and thin-film $\text{PbMg}_{1/3}\text{Ta}_{2/3}\text{O}_3$ and $\text{PbSc}_{0.5}\text{Ta}_{0.5}\text{O}_3$ have not shown a noticeable dependence of polar phonon structure on degree of chemical ordering either. Also polycrystalline ceramic-type PMN films prepared by chemical solution deposition have been found to behave similarly to bulk PMN.⁹ The fast dipoles with the frequency marked as E in Fig. 5 are characteristic for the physically grown epitaxial or polycrystalline films, but are not directly connected to epitaxial quality or degree of chemical ordering. The common microstructural feature of such films is their two-dimensional in-plane clamping by the substrate: either the whole single-crystal epitaxial film or vertical columnar crystallites growing from the bottom to the top of the polycrystalline film are clamped. As follows from studies of strained PMN films,¹⁴ the in-plane thermal strain developing during measurements (estimated 0.04% in PMN/MgO system) cannot noticeably affect zero-field dielectric properties. The mechanism through which the film-substrate coupling might lead to formation of the fast dipoles is unclear and requires further investigations.

In summary, the low-frequency intrinsic dielectric response and the response in far-infrared frequency range of epitaxial PMN films are experimentally studied and analyzed. The response is interpreted as that of paraelectriclike matrix and dipoles, with the dipolar volume fraction exponentially growing on cooling. Compared to single-crystal PMN in PMN films, the dipolar relaxation time spectra contain larger fractions of fast relaxators, which increase with decreasing film thickness. This is shown to explain the enhanced RE behavior in the films. The film-substrate coupling might be responsible for the peculiar fast dipoles.

The authors are thankful to J. Petzelt and J. Hlinka for valuable discussions and creative criticism of the manuscript. In part, the work was supported by Academy of Finland (Project No. 118250), Czech Science Foundation (Project No. 202/09/0682), and Czech Academy of Science (AVOZ10100520).

*Corresponding author; marinat@ee.oulu.fi

¹Z. Kutnjak, J. Petzelt, and R. Blinc, *Nature (London)* **441**, 956 (2006); G. Xu, J. Wen, C. Stock, and P. M. Gehring, *Nat. Mater.* **7**, 562 (2008).

²M. Tyunina, M. Plekh, and J. Levoska, *Phys. Rev. B* **79**, 054105 (2009).

³A. A. Bokov, Y.-H. Bing, W. Chen, Z.-G. Ye, S. A. Bogatina, I. P. Raevski, S. I. Raevskaya, and E. V. Sahkar, *Phys. Rev. B* **68**, 052102 (2003).

⁴V. Bovtun, S. Kamba, A. Pashkin, M. Savinov, P. Samoukhina, J. Petzelt, I. P. Bykov, and M. D. Glinchuk, *Ferroelectrics* **298**, 23 (2004).

⁵S. Kamba, M. Kempa, V. Bovtun, J. Petzelt, K. Brinkman, and N. Setter, *J. Phys.: Condens. Matter* **17**, 3965 (2005).

⁶S. Kamba, D. Nuzhnyy, S. Veljko, V. Bovtun, J. Petzelt, Y. L. Wang, N. Setter, J. Levoska, M. Tyunina, J. Macutkevici, and J. Banys, *J. Appl. Phys.* **102**, 074106 (2007).

⁷M. Tyunina and J. Levoska, *Phys. Rev. B* **72**, 104112 (2005).

⁸B. Sareni, L. Krähenbühl, A. Beroual, and C. Brosseau, *J. Appl. Phys.* **80**, 1688 (1996), and references therein.

⁹V. Bovtun, S. Veljko, S. Kamba, J. Petzelt, S. Vakhruhev, Y. Yakymenko, K. Brinkman, and N. Setter, *J. Eur. Ceram. Soc.* **26**, 2867 (2006).

¹⁰T. R. Yang, S. Perkowitz, G. L. Carr, R. C. Budhani, G. P. Williams, and C. J. Hirschmugl, *Appl. Opt.* **29**, 332 (1990).

¹¹S. Wakimoto, C. Stock, R. J. Birgeneau, Z.-G. Ye, W. Chen, W. J. L. Buyers, P. M. Gehring, and G. Shirane, *Phys. Rev. B* **65**, 172105 (2002).

¹²J. Levoska, M. Tyunina, A. Sternberg, and S. Leppävuori, *Ferroelectrics* **271**, 137 (2002).

¹³S. Kamba, M. Berta, M. Kempa, J. Hlinka, J. Petzelt, K. Brinkman, and N. Setter, *J. Appl. Phys.* **98**, 074103 (2005).

¹⁴M. Tyunina and J. Levoska, *J. Appl. Phys.* **97**, 114107 (2005).